Dual closed-loop, optoelectronic, auto-oscillatory detection circuit for monitoring fluorescence lifetime-based chemical sensors and biosensors

Emmanuil Rabinovich
University of New Mexico
Center for High Technology Materials
1313 Goddard, SE
Albuquerque, NM 87106

Tengiz Sviminoshvilli
Michael J. O'Brien
University of New Mexico
Department of Chemical and Nuclear Engineering
Farris Engineering Center #209
Albuquerque, NM 87131

Steven R. J. Brueck
University of New Mexico
Center for High Technology Materials
1313 Goddard, SE
Albuquerque, NM 87106

Gabriel P. Lopez
University of New Mexico
Department of Chemical and Nuclear Engineering
Farris Engineering Center #209
Albuquerque, NM 87131
E-mail: gplopez@unm.edu

Abstract. We present a new detection instrument for sensor measurements based on excited-state fluorescence lifetimes. This system consists of a primary optoelectronic loop containing a resonance-type rf amplifier, a modulatable fluorescence-excitation light source, a fiber optic feedback loop (with a gap for a fluorescent sensor), and a photomultiplier tube. A secondary, phase-feedback optoelectronic circuit consists of a long-wavelength-pass optical filter, a second photomultiplier tube, a photodiode, an electronic phase detector, a dc amplifier, and an electronic phase shifter (inserted into the main loop). This phase-feedback circuit is new with respect to our previous work. Under the appropriate conditions, the main loop exhibits self-oscillations, manifesting themselves as sinusoidal rf modulation of light intensity. The phase-feedback circuit detects the modulation phase shift resulting from the finite excited-state lifetimes of a fluorophore. As the excited state lifetime changes, the phase shift from the electronic phase shifter also changes, which results in a shift in self-oscillation frequency. The detection system uses self-oscillation frequency as the detection parameter and has excellent resolution with respect to changes in excited-state lifetime ($\sim$1 ps). © 2004 Society of Photo-Optical Instrumentation Engineers. [DOI: 10.1117/1.1688814]

Keywords: closed loop; self-oscillations; biosensors; chemical sensors; fluorescence lifetime.

Paper 03037 received Apr. 1, 2003; revised manuscript received Aug. 14, 2003; accepted for publication Sep. 4, 2003.

1 Introduction

Steady state and time-resolved fluorescence spectroscopy are major research tools in the development of chemical and biological sensor systems, with numerous applications in the biomedical technology, including drug discovery, diagnosis, and preventative-health applications (through monitoring of environmental toxins, for example). Fluorescence-based detection modalities have the potential for high sensitivity and offer a large choice of fluorescence sensor techniques.[1] Their high sensitivity has driven the development of a variety of fluorescence-based sensors.[2] Steady state (intensity-based) fluorescence measurements are relatively simple to implement, but are sensitive to spurious factors such as fluctuations in excitation light intensity, bleaching of fluorophores, and changes in dye concentrations.[3] An alternative is time-resolved (lifetime-based) fluorescence spectroscopy, which has reduced sensitivities to these effects.[3] Unfortunately, sensor systems employing time-resolved spectroscopic techniques tend to be complex[4] and expensive.

There are two branches of time-resolved spectroscopy: time-domain and frequency-domain techniques.[4] Time-domain techniques measure the decay of fluorescence intensity after a short (typically nanosecond or picosecond dura-

tion) pulse of excitation light. Frequency-domain techniques (also known as modulation spectroscopy) rely instead on detecting changes in light intensity modulation depth and/or intensity modulation phase shifts caused by the finite excited state lifetime of a fluorophore.[3,4]

Attempts have been made to create simple and inexpensive chemical and biosensor platforms using frequency-domain spectroscopic techniques, such as single-frequency phase fluorimeters.[3,5,6] More recently, a new detection platform design based on a self-oscillating, optoelectronic closed-loop system was presented.[7,8]

The term "closed loop" can be applied to a number of systems that are quite different from ours, including at least one for frequency-domain fluorimetry.[9] To avoid confusion, in the context of this paper we define a closed-loop optoelectronic system as one consisting of an rf amplifier, a modulatable light source (such as an LED or laser diode), a delay line (such as a fiber optic delay line, for instance), and a photodetector. The signal from the output of the amplifier modulates the output intensity of the light source. The modulated light passes through the delay line and is converted back into an electrical signal by the photodetector. This electrical signal enters the input of the amplifier. When the combined gain of the amplifier and photodetector is large enough to offset the optical and electrical signal losses in the loop, the system

Address all correspondence to Gabriel P. Lopez. University of New Mexico, Department of Chemical and Nuclear Engineering, 1313 Goddard, SE Albuquerque, NM 87106. E-mail: gplopez@unm.edu

manifests self-oscillations in the form of sinusoidal intensity modulations of light.[8,10–12]

The earliest sensor applications of closed-loop systems have been in vibration sensing systems.[11,12] Only recently have they been applied to time-resolved spectroscopy, where a fluorescent sensor and a long-wavelength-pass optical filter have been inserted into the delay loop.[8] In such a scheme, the intensity-modulation phase shift (caused by the finite excited-state lifetime) of the fluorescent sensor enables the sensor to serve as a phase shifter inside the loop. As the modulation phase shift changes, the frequency of the loop's self-oscillations also changes. The frequency serves as the detection parameter of the sensor platform. Experiments have shown that the noise levels of these systems, which are constructed from relatively inexpensive components, can correspond to uncertainties in lifetime changes of the order of a picosecond.[8]

An acknowledged challenge to the application of closed-loop systems to time-resolved fluorescence spectroscopy applications has been in meeting the gain condition.[8] In a previously described configuration, a long-wavelength-pass optical filter was required to prevent excitation light from entering the second part of the loop (leading to the photodetector). It was difficult to obtain self-oscillations in the prototype when using weak fluorophores, as the fluorescence yield and the loss of intensity-modulation depth (caused by the finite fluorescence lifetime[3]) are sources of signal loss.

Weak fluorophores could be dealt with by using improved gain in the closed loop, but there are practical limits. Increasing the electronic gain too greatly results in increased electronic noise and therefore increased bandwidth of self-oscillations, degrading the precision of the frequency counting method. A scheme that retains the advantages of the optical feedback without requiring as much electronic gain would be advantageous in some cases.

In this work, we chose to remove the optical filter from the main loop. This enabled the excitation light to reach the photodetector, reducing a significant portion of the optoelectronic circuit's losses. This, however, necessitated a new mechanism for introducing a lifetime-dependent phase shift in the loop, since the fluorescence excitation light is frequently significantly stronger than the fluorescence emission light.

Our solution was to map the intensity modulation phase shifts in the fluorescence emission light into an electronic phase shift. This is accomplished with a secondary, phase-feedback circuit containing an electronic phase detector and a voltage-controlled electronic phase shifter (VCEPS). The output of the phase detector is a dc voltage dependent on the modulation phase shift of the fluorescence emission light and was used to control the VCEPS. The VCEPS was placed within the optoelectronic circuit, providing the necessary lifetime-dependent phase-shifting mechanism. While this solution significantly increased the complexity of the design, the electronic phase-shifting mechanism, driven by the modulation phase shift of the fluorescence emission, created less signal losses in the main loop. Changes in fluorescence phase shifts still altered the resonant frequency of the main loop.

As the excited-state fluorescence lifetime changed, the rf intensity-modulation phase shift of the fluorescence emission changed. Thus, the phase difference between inputs of the electronic phase detector changed, which caused the phase

shift of the VCEPS to change, altering the frequency of self-oscillations until a new equilibrium condition was reached.

The detection system presented here could be used for chemical or biosensor molecular transduction methods that result in a deterministic change in the excited state lifetime of a fluorescent probe. These include methods based on fluorescence resonance energy transfer[13,14] or quenching[13,15] of fluorescent probes.

2 Prototype Design Specifics

2.1 Main Feedback Loop

The new configuration of the closed-loop system, with the secondary phase-feedback optoelectronic circuit, is shown in Fig. 1. The resonance amplifier is an RTA-500098 rf amplifier [Radar Technology Inc. RTA-500098 with central frequency 45 MHz, bandwidth (3 dB) 5.2 MHz, 75-dB maximum (variable) gain, and 2.8-dB noise figure]. The phase shift of the amplifier itself can be approximated as constant with respect to changes in modulation frequency.[8] We chose a narrow-bandwidth amplifier to suppress the generation of higher order harmonics in the main loop (the changes in frequency that we observe are much less than the bandwidth of this amplifier). The output of the amplifier is connected to the ac input of a bias-T circuit (ZFBT-6GW 09809, Mini-Circuits, Inc.). The dc input of the bias-T circuit is connected to a dc current supply (LDC 500, Thor Labs, Inc.). The output of the bias-T circuit is connected to the modulatable fluorescence excitation light source.

The fluorescence excitation light source is a blue LED (NSPB500S, Nichia America Corp., 3-mW output power, peak wavelength of 460 nm). This LED can be used[16] with modulation frequencies at least as high as 250 MHz. The fiber optic delay line consists of two pieces of multimode fiber (Thor Labs, Inc.). Each piece of fiber is 4.4 m long and has a diameter of 600 μm. A cuvette containing a fluorescent sensor is placed between the two fiber optic pieces. Light is coupled into each fiber with a fiber-optic collimator. The primary loop's photodetector is an ultracompact PMT (model R5600, Hamamatsu Corp.). The electrical output of this PMT feeds into the input of a VCEPS (SO-03-411, Pulsar Microwave Corp.). The output of the VCEPS connects to the input of the resonance amplifier, closing the loop.

2.2 Secondary (Phase Feedback) Loop

A long-wavelength-pass optical filter (LP-530, CVI Laser, Inc.) is placed on the side of the cuvette (i.e., not in-line with the primary loop, as shown in Fig. 1). Only fluorescence emission light will pass through the filter to enter a large fiber bundle (bundle diameter ≈ 1 cm). The fiber bundle feeds into a second PMT (ultracompact model R5600 PMT, Hamamatsu Corp.). The signal from this second PMT enters a series of two ZFL-1000 amplifiers and a (passive) bandpass filter (BIF-40 filter, Mini-Circuits, Inc., center band frequency 42 MHz, <1 dB loss passband bandwidth ≈ 14 MHz). The amplified signal passes into one input of the electronic phase detector.

A second blue LED is connected in parallel with the fluorescence excitation source, but is pointed away from the main loop, toward a photodetector (PDA153 high-speed photodetector, Thor Labs, Inc.). This setup provides a reference signal

Fig. 1 Schematic of the dual-loop system. The primary loop consists of the resonance amplifier, bias-T, excitation light source, fiber optic delay line, photomultiplier tube (PMT), and VCEPS. The phase feedback mechanism (secondary loop) consists of half of the fiber optic loop (L') and the components shown inside the primary loop.

to the secondary loop that is electrically isolated from the main loop. Coaxial cable directs the signal output of this second photodetector to an rf amplifier (ZFL-1000 942 6-01, Mini-circuits, Inc.). This amplifier's output connects to the second input of the electronic phase detector (ZRPD-1, Mini-Circuits, Inc.) and to a frequency-counting unit (discussed shortly).

The output of the electronic phase detector is connected to a variable-gain, basic inverting dc amplifier,[17] based on a 741 op amp (Radio Shack, Inc.). The gain range of this amplifier is 1 to 100, but we operated with a gain of 5. The dc output of this amplifier connects to the control input of the VCEPS. The amplifier contains an integrated voltage follower,[17] based on another 741 op amp.

2.3 *Frequency-Counting Mechanisms*

We used a computer-based frequency counter. We constructed this with a computer (PC, Pentium II, 300 MHz), a digital acquisition (DAQ) board (AT-MIO-16-E1, National Instruments, Inc., with a 1-MHz sampling rate and 64 analog inputs) and frequency-analysis software, custom-written with LabVIEW 6i (National Instruments, Inc.). This software is based on the mathematics of discrete Fourier transforms[18] (DFTs). Such computer-based mechanisms can be cost-effective, perform well, and are inherently scalable for sensor array applications.[5,7]

With the computer-based frequency counter, the DAQ board first acquires a discrete time series (DTS). The computer performs a fast-Fourier transform (FFT) of the DTS,

discards the second half of the FFT (to avoid the effects of aliasing)[18] and modulus-squares each term to obtain a power spectrum.

The computer fits the peak of the power spectrum with a second- or third-order polynomial to determine the frequency-space location of the peak more precisely. The fitting routine is necessary to reduce the effects of noise in the power spectrum. The location of the fit's maximum is determined through the first-order derivative, and multiplied by a constant (dependent on the sampling rate and number of elements in the DTS) to yield the peak frequency in the power spectrum.

Because systems employing DFTs can resolve only frequencies less than or equal to half of the sampling frequency,[18] this unit is capable of measuring frequencies only between 0 and 500 kHz. We therefore must downshift the frequency of self-oscillations in the loop (which is typically of the order of 40 to 50 MHz) before the computer-based frequency counter can be used for relative measurements. We achieve this with a mixer (ZFM-1W, Mini-Circuits, Inc.) and a digital signal synthesizer (HP 8648B, Hewlett Packard, Inc.). The output passes through a low-frequency-pass electronic filter (Kiwa Electronics, Inc. passive, low-pass filter, with a 500-kHz cutoff frequency) before entering the DAQ board.

3 Gain and Phase Conditions for Dual-Loop Optoelectronic Circuit

The dual-loop optoelectronic circuit begins to self-oscillate if two conditions are met. First, the round-trip signal gain must

be increased to equal the round-trip losses of the loop. Second, the total phase shift in a single round trip must be a multiple of 2π.

The latter requirement is known as the phase condition, and can be expressed for our system as

$$n\frac{L}{c}\Omega+\Phi_{amp}+\Phi_{LED}+\Phi_{PMT1}+\Phi_{PS}(\Omega,\tau)=2\pi N, \quad (1)$$

where L is the total length of the fiber optic delay line, c is the speed of light in vacuum, n is the refractive index of the fiber delay line, Ω is the modulation frequency (in radians per unit time), τ is the excited-state fluorescence lifetime, and N is any integer. Also Φ_{amp}, Φ_{LED}, and Φ_{PMT1} are the discrete phase shifts introduced by the resonance amplifier, the LED, and the primary PMT, respectively. These are, of course, independent of fluorescence lifetime and can be assumed to be independent of Ω; $\Phi_{PS}(\Omega,\tau)$ is the phase shift introduced by the VCEPS.

Since the phase shift of the fluorescence emission intensity modulation is given by arctan($\Omega\tau$), assuming a single-exponential decay rate,[3] and it is this phase shift that ultimately causes the frequency response of the system to lifetime changes, it is desirable to choose a working frequency, Ω_0, in the vicinity of $1/\tau$ to maximize the phase response to changes in lifetime. With this frequency, one can use Eq. (1) to calculate the desired value of L in the absence of a fluorophore, and to choose the frequency range of the electronic components (such as the resonance amplifier).

If Φ_{PS} is a linear function of the phase detector voltage (V_{PD}) over a certain range of its values, it can be approximated as

$$\Phi_{PS}=a_1 V_{PD}+b_1, \quad (2)$$

where a_1 and b_1 are constants determined from the phase shifter calibration curve. The dc output from the phase detector V_{PD} depends on the phase difference between the two input rf signals:

$$\Delta\Phi_{PD}=\Phi_1-\Phi_2, \quad (3)$$

where Φ_1 and Φ_2 are the phases of the rf signals at the phase detector inputs 1 and 2, respectively. These are expressed as

$$\Phi_1=\Phi_{LED}+n\frac{L'}{c}\Omega+\arctan(\Omega\tau)+n_{FB}\frac{L_{FB}}{c}\Omega+\Phi_{PMT2}$$
$$+\Phi_{RFA1}+\Phi_{RFA2}+\Phi_{BPF}+n_c\frac{l_1}{c}\Omega, \quad (4a)$$

$$\Phi_2=\Phi_{LED}+\Phi_{PD}+\Phi_{RFA3}+n_c\frac{l_2}{c}\Omega, \quad (4b)$$

where Φ_{LED} is the discrete phase shift introduced by an LED, n is as already defined, L' is the length of the part of the fiber optic delay line that carries excitation light to the fluorescent sample (typically half of L), n_{FB} is the index of refraction of the collection fiber bundle, L_{FB} is the length of the fiber bundle, Φ_{PMT2} is the discrete phase shift introduced by PMT2, Φ_{RFA1} and Φ_{RFA2} are the discrete phase shifts introduced by the broadband rf amplifiers following PMT2, Φ_{BPF}

is the discrete phase shift introduced by the passive bandpass filter, n_c is the square root of the coaxial cable's normalized dielectric constant ($\varepsilon/\varepsilon_0$), l_1 is the net length of the coaxial cable connecting PMT2 to the electronic phase detector (including the cable connecting the intermediate two rf amplifiers and bandpass filter), Φ_{PD} is the discrete phase shift introduced by the photodetector, Φ_{RFA3} is the discrete phase shift of the broadband amplifier following the photodetector, and l_2 is the net length of the coaxial cable from the photodetector to the broadband rf amplifier and from the rf amplifier to the electronic phase detector.

If V_{PD} is a linear function of a certain range of $\Delta\Phi_{PD}$ we can approximate it as

$$V_{PD}=\beta(a_2\Delta\Phi_{PD}+b_2), \quad (5)$$

where a_2 and b_2 are determined from the linear part of the phase detector calibration curve; and β is the gain of an external dc amplifier connected to the output of the phase detector, which can be adjusted for tuning purposes.

For convenience, we define the following quantities:

$$\Phi_{k_1}\equiv(\Phi_{amp}+\Phi_{LED}+\Phi_{PMT1}+b_1),$$

$$\Phi_{k_2}\equiv[a_1 b_2+a_1 a_2(\Phi_{PMT2}-\Phi_{PD}+\Phi_{RFA1}+\Phi_{RFA2}-\Phi_{RFA3})],$$

such that Φ_{k_1} represents the net discrete phase shifts of the optoelectronics in the primary loop, Φ_{k_2} represents the net discrete phase shifts of the optoelectronics in the secondary loop, and l_c represents the difference in coaxial cable lengths from both inputs of the electronic phase detector. For simplicity, we assume that Φ_{k_1} and Φ_{k_2} are approximately constant with respect to changes in Ω.

Combining Eqs. (1) through (5) and rearranging terms enables us to derive the following expanded phase condition:

$$2\pi N=\Phi_{k_1}+\beta\Phi_{k_2}+\beta a_1 a_2\arctan(\Omega\tau)+\left(\frac{\Omega}{c}\right)$$
$$\times[nL+\beta a_1 a_2(nL'+n_c l_c+n_{FB}L_{FB})]. \quad (6)$$

3.1 Frequency Response to Changes in Lifetime

We are interested in the relationship between small changes in the self-oscillation frequency of the system ($d\Omega$) and small changes in fluorescence lifetime ($d\tau$). Taking the derivative of Eq. (6) and rearranging terms leads to

$$\frac{d\Omega}{\Omega}=\frac{d\tau}{\tau}\left\{\frac{g(\Omega\tau)}{(\Omega nL)/(c\beta a_1 a_2)-[(\Omega/c)(nL'+n_c l_c+n_{FB}L_{FB})+g(\Omega\tau)]}\right\}, \quad (7)$$

where $g(\Omega\tau)\equiv(\Omega\tau)/[1+(\Omega\tau)^2]$. Note that, for the sake of simplicity, we have neglected the lengths of the coaxial cables connecting PMT1 to the VCEPS, the VCEPS to the resonance amplifier, and the resonance amplifier to the LEDs, assuming that their total length was significantly less than L. Should this not be the case, the effects of these cable lengths can be reintroduced with the following substitution:

$$nL \rightarrow (nL + n_c l_c'),$$

where l_c' is the net length of these cables.

It is interesting to examine Eq. (7) for two limiting cases. As the magnitude of β approaches infinity, the first term in the denominator of Eq. (7) goes to zero. This term represents the primary loop in the dual-loop circuit. Therefore, for very large values of the dc amplifier gain, the frequency response of the system is dominated by the secondary loop. As β goes to zero, $d\tau$ and $d\Omega$ become decoupled. This is to be expected, since setting β to zero is equivalent to removing the phase feedback mechanism, which would be the same as our previous configuration without the long-wavelength-pass optical filter.

3.2 System Stability

A primary source of instability in the system can be attributed to slow variations of the phase constant terms of Eq. (6), Φ_{k_1} and Φ_{k_2}. While these terms may not vary with Ω, they may vary with other environmental variables. For instance, a change in the operational temperature of the resonance amplifier could change Φ_{amp}. This would result in a change of Ω when τ remains constant, introducing errors into the measurements of reaction kinetics.

To find the effects of small changes of Φ_{k_1} and Φ_{k_2} on Ω, we take the partial derivatives of Eq. (6) and combine them according to error analysis rules, arriving at

$$\frac{\delta\Omega}{\Omega} = \frac{[(\delta\Phi_{k_1})^2 + \beta^2(\delta\Phi_{k_2})^2]^{1/2}}{(\Omega/c)nL + a_1 a_2 \beta[(\Omega/c)(nL' + n_c l_c + n_{FB}L_{FB}) + g(\Omega\tau)]},$$
$$(8)$$

where $\delta\Omega$, $\delta\Phi_{k_1}$, and $\delta\Phi_{k_2}$ represent the uncertainty levels of Ω, Φ_{k_1}, and Φ_{k_2}, respectively. These are, of course, unsigned quantities. A similar calculation can be performed for the phase condition of the single-loop system,[8] resulting in

$$\frac{\delta\Omega}{\Omega} = \frac{\delta\Phi_{k_1}}{(\Omega/c)nL + g(\Omega\tau)}.$$
$$(9)$$

Comparisons of Eqs. (8) and (9) show two important points. First, the secondary, phase-feedback loop has the capability of reducing frequency drift caused by variations in time of Φ_{k_1}. With the appropriate choice of magnitude and polarity of $(a_1 a_2 \beta)$, the secondary loop's presence will increase the denominator of Eq. (8), decreasing $(\delta\Omega/\Omega)$ compared to Eq. (9). However, the secondary loop makes the system much more complex, and adds a factor (Φ_{k_2}) to the numerator of Eq. (8) due to the new optoelectronic components. We would expect that the contribution of Φ_{k_2} would be relatively small, though, since only Φ_{k_1} contains terms dealing with the resonance amplifier.

The secondary phase-feedback loop should also reduce noise. Equation (6) contains two terms that have dependence on Ω: the fluorophore term $[\beta a_1 a_2 \arctan(\Omega\tau)]$ and the delay line term $\{(\Omega/c)[nL + \beta a_1 a_2(nL' + n_c l_c + n_{FB}L_{FB})]\}$. If τ remains constant, a small change in Ω will change the phase of the delay line term and require the fluorophore term to change as well to compensate until an equilibrium. The key,

however, is the gain $(\beta a_1 a_2)$ of the fluorophore term. We can select the magnitude and sign of the gain to enable the two terms to balance out more quickly with the net result that the system has lower noise. In the previous single-loop design, the "gain" of the fluorophore term was fixed in magnitude and sign. Disconnecting the phase-feedback loop completely in the new design $(\beta = 0)$ would leave only the delay line term dependent on Ω, so that noise in the system would be much larger.

4 Experiment

We selected the pH-sensitive fluorescent dye, carboxy semi-naphthofluorescein (SNAFL-2, Molecular Probes, Inc) for our experiments. Changes in the pH of a solution containing this dye trigger substantial lifetime changes, which can result in measurable frequency shifts of the system. This dye has been used previously as a model chemical sensor for lifetime-based detection platforms.[5,8] We chose initial pH values of 9.2 since previous findings indicated[5] that that would yield the maximum changes in lifetime for a given change in pH.

4.1 Calibration of Phase Detector and VCEPS

To determine the a_1 and a_2 parameters required for estimates involving Eq. (7), we generated calibration curves for both the electronic phase detector and the VCEPS using two digital signal generators (HP 8648B, Hewlett Packard, Inc.), two rf mixers (ZFM-150, Mini-Circuits, Inc.), a variable dc power supply, a digital voltmeter, and a custom-built multichannel phase meter that is described elsewhere.[5] Both digital signal generators shared a common clock, so their output phases were locked to each other.

4.1.1 VCEPS calibration

The first signal generator was set to 50.00009 MHz. The signal from the first signal generator was split and connected to a mixer and the VCEPS rf input. The rf output of the VCEPS was connected to the second mixer. The dc power supply was connected to the control input of the VCEPS.

The second signal generator was set to 50 MHz to provide a heterodyne signal. Its output was split and directed to the mixers. The difference signal from the mixers was 90 Hz, which was connected to the low-frequency inputs of the phase meter. We varied the control voltage between 0 and 18 V while measuring the phase difference in the 90-Hz signals. We repeated the experiment twice, once with the synthesizers set to 45.00009 and 45 MHz, and once more with the synthesizers set to 40.00009 and 40 MHz. The results are shown in Fig. 2. The values of a_1 and b_1 from Eq. (2) for the 40-MHz run were, respectively, -8.94 ± 0.26 deg/V and 392.34 ± 0.25 deg. These values were required to calibrate the phase detector.

4.1.2 Phase detector calibration

Once the phase shifter was calibrated, it was a simple matter to use it to calibrate the phase detector. We connected one of the HP digital frequency synthesizers to the rf input of the VCEPS. The control input of the VCEPS was connected to the variable-voltage dc power supply. The output of the VCEPS fed into one of the inputs of the electronic phase detector. We connected the second frequency synthesizer to
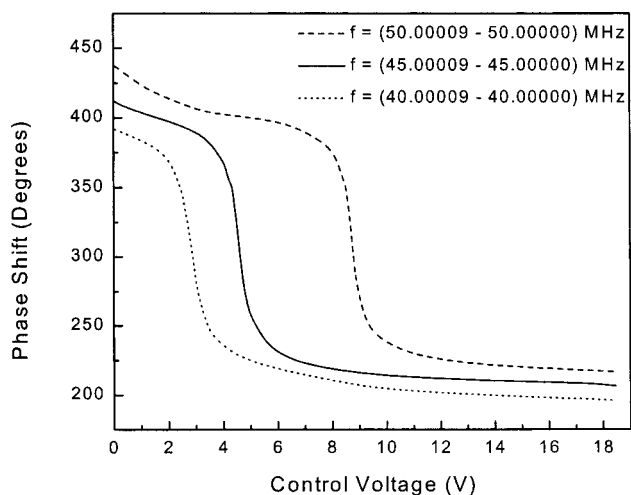
Fig. 2 Calibration curves for the VCEPS.

the other input of the electronic phase detector, and connected the (dc) output of the electronic phase detector to a digital voltmeter.

The two signal generators were set to output sinusoidal waveforms with a 40-MHz frequency and a 700-mV amplitude. The control voltage was varied between 0 and 1.6 V while we recorded the output voltage of the phase detector. Using the calibration curve for the VCEPS, we translated the phase shifter input voltage into a phase shift. The phase detector output versus input phase shifts are shown in Fig. 3. A linear fit indicates that the constants a_2 and b_2 in Eq. (5) are -11.45 ± 0.17 mV/deg and 4407.46 ± 64.45 mV, respectively.

4.2 System Response to Changes in pH

We poured 3 ml of a pH 9.2 solution containing SNAFL-2, deionized (DI) water, and sodium hydroxide into a cuvette and placed it within the gap between the two parts of the optical delay line (as shown in Fig. 1). We connected an oscilloscope and spectrum analyzer to the output of the photodetector. This enabled us to monitor the self-oscillations manifesting themselves as intensity modulation of the fluorescence
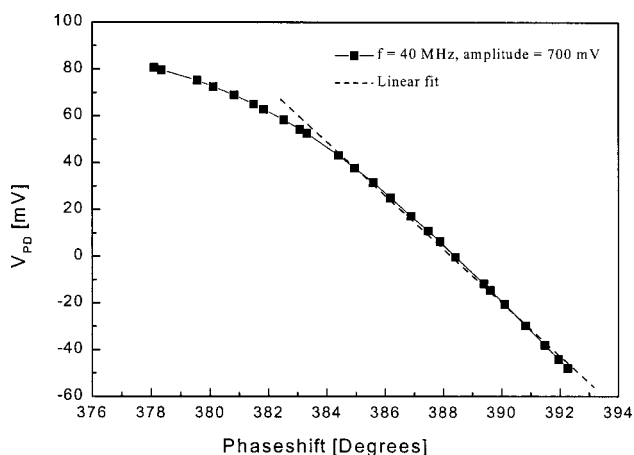
Fig. 3 Calibration curve for the electronic phase detector.
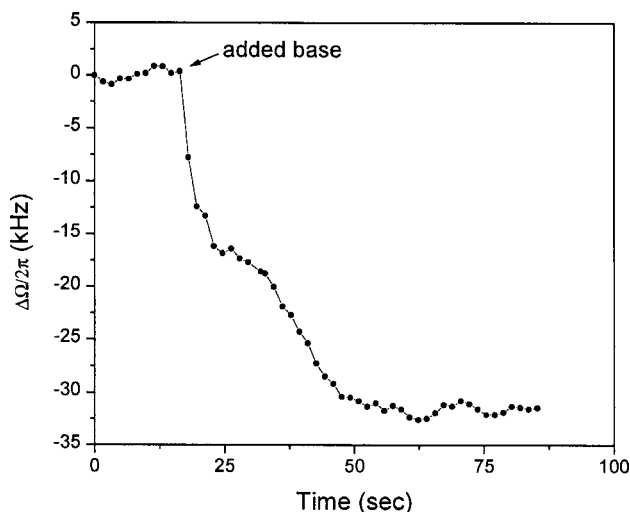
Fig. 4 Experimental data from the pH sensor experiment. The addition of pH 12 NaOH solution to the cuvette alters the pH from 9.2 to 9.64, resulting in a change in the frequency of the system's self-oscillations of 32 kHz.

excitation light. We powered on the system and adjusted the primary loop PMT1 voltage (257 V) and amplifier gain until self-oscillations were obtained in the system.

We then connected the oscilloscope and spectrum analyzer to the output of the secondary loop PMT (PMT2). This enabled us to monitor the rf signal from the intensity-modulated fluorescence emission light. The PMT voltage was slowly increased from zero until the amplitude of the signal was ~100 mV.

We connected the computer-based frequency counter assembly (including the heterodyne circuitry) to the output of the photodetector. We adjusted the frequency of the digital signal synthesizer so that the downshifted signal was near the center of the DAQ frequency resolution range (~250 kHz). The system was allowed to stabilize for a few minutes before we began recording data with the computer-based frequency counter. We added 10 μl of 0.1 N aqueous NaOH (measured pH 12.1 with pH meter) solution to the cuvette. This caused a frequency shift ($\Delta\Omega/2\pi$) of 32 kHz, as can be seen in Fig. 4. Note that the frequency shift due to the increasing pH in Fig. 4 is negative, whereas it has previously been shown to be positive in the single-loop system.[8] This is due to the heterodyning of the signal. While the actual resonance signal may have increased, the difference signal would decrease if the frequency synthesizer were set to a frequency higher than the resonant loop signal.

We used a pH meter on the solution after the experiment and found the final pH level to be 9.64. According to published data,[6] a pH shift of 0.44 should produce a phase shift in the SNAFL of about -5 deg. This neglects the frequency dependence of the fluorophore's phase shift but should be suitable for a rough check of the prototype's response compared to theory. Replacing $\arctan(\Omega\tau)$ in Eq. (6) with $\Phi_{\text{fluorophore}}$ leads to

$$(\Delta\Phi_{\text{flourophore}})(\beta a_1 a_2) = -\left(\frac{\Delta\Omega}{c}\right)[nL + \beta a_1 a_2(nL' + n_c l_c + n_{\text{FB}} L_{\text{FB}})].$$

This equation predicts a frequency change of about 114 kHz. The value observed (32 kHz) is well within an order of magnitude. Unfortunately, the necessity to remove the solution and test it with a pH meter meant that we could not demonstrate the reversability of the pH sensor with 0.1 N HCl acid, as we had done previously with the single-loop system.[8] However, a similar demonstration of reversability with the new configuration has been shown with preliminary results elsewhere.[19]

4.3 Stabilization Effects of the Phase-Feedback Circuit

As already stated, the equation relating the uncertainty levels of Ω to the uncertainty levels of the optoelectronic-based phase constants in the loop has terms that have the potential to both increase and decrease $\delta\Omega/\Omega$ relative to the simpler single-loop system. We expect that the decreasing term will dominate, producing a net decrease in $\delta\Omega/\Omega$. To test this, we compared Ω over time with and without connecting the secondary phase-feedback loop to the phase shifter. Disconnecting the secondary loop is equivalent to letting $\beta \rightarrow 0$ in Eq. (7). Comparison of the signals with and without the phase-feedback loop will demonstrate whether or not the contribution of $\delta\Phi_2$ in Eq. (8) is greater than that of $a_1 a_2 [(\Omega/c)(nL' + n_c l_c + n_{FB} L_{FB}) + g(\Omega \tau)]$. For the components used in our system, the value of $(\Omega nL)/c$ is approximately 4π and the value of $g(\Omega \tau)$ is of the order of 1 (for the fluorophore we selected[8]); this experiment should provide a rough comparison between the newer configuration and the older single-loop design.

We placed a cuvette containing SNAFL-2 solution in the system, with the secondary phase-feedback loop connected ($\beta \neq 0$). We adjusted the PMT and amplifier gains as described above and allowed the system to stabilize before starting to record data with the computer-based frequency counter. The results are shown in Fig. 5(a). The signal noise level ($\delta\Omega/2\pi$), as determined by standard deviation, was 368.3 Hz. Using Eq. (7), we estimate $\delta\tau$ at 1 ps. For comparison purposes, a Fluorolog 3 (with τ-3 module) commercial spectrofluorometer (Instruments S.A., Inc.) in our laboratory has a lifetime change resolution of 10 ps.

We then disconnected the secondary loop ($\beta = 0$) and repeated the measurements. At no time did we attempt to induce changes in lifetime by adding HCl or NaOH. The results are shown in Fig. 5(b). The system demonstrated roughly $2.6\times$ larger noise levels (standard deviation = 964.1 Hz) when the secondary loop was disconnected. The overall signal drift values were larger as well.

4.4 Lower Limit of Noise Levels

In our experience, a dominant factor in the system's stability is the losses of the (primary) loop. Decreasing the losses in the loop enables one to use smaller gains in the PMT and resonance amplifier, which result in sharper profiles in frequency space and smaller fluctuations in peak frequency. Indeed, the primary motivation in the development of the new system was to enable us to remove the long-wavelength-pass filter from the primary loop and thereby reduce the losses. However, these factors cannot be accounted for in the equa-
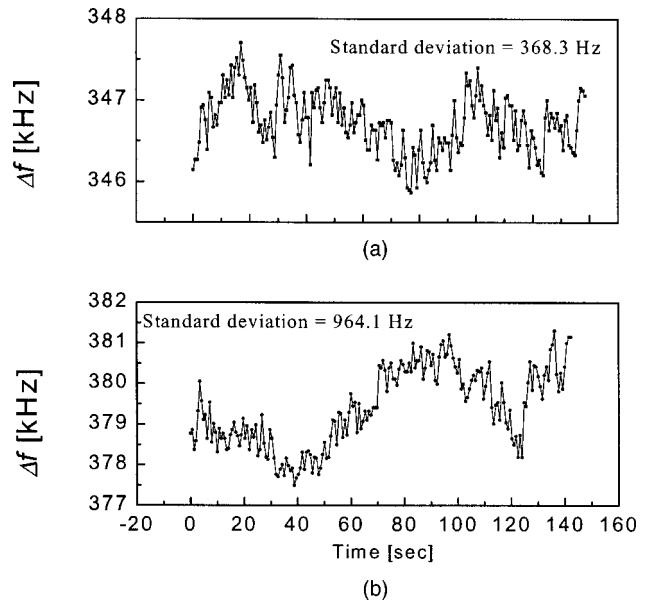

Fig. 5 Results from stability experiment (a) with the phase-feedback mechanism and (b) without the phase-feedback circuit (comparable to the simpler, single-loop design). The phase-feedback mechanism increases stability. Standard deviations of the data are included in the plots.

tions presented here. We expect that reduction of the losses of the loop will enable us to estimate the ultimate noise limits of the new system.

To determine the best signal-to-noise level achievable with the dual-loop system, we eliminated the gap between the two portions of the fiber delay line and connected their ends. This, of course, left no room for a fluorophore in a cuvette, so no fluorophore was used. The secondary phase-feedback loop was connected and powered, but had no optical input.

Again, the system was powered on, the gains of the resonance amplifier and PMT1 were adjusted, and self-oscillations were obtained. After stabilizing the system, we began to record data with the computer-algorithm-based frequency counter. The results are shown in Fig. 6. As expected, the signal noise level improved (standard deviation = 251.2 Hz).

The implications of this experiment are that further improvement in signal noise levels will result if the current system is modified to reduce signal losses in the main loop. For example, laser diodes could be used (rather than LEDs) as fluorescence excitation light sources since they have better modulation-depth characteristics and can couple light into fibers more efficiently.

5 Discussion

We presented a new configuration of a closed-loop, auto-oscillatory, optoelectronic system for chemical and biosensor measurements. This system, like its predecessor, has been designed to oscillate at rf frequencies, which are dependent on the excited-state lifetime of a fluorescent chemical or biosensor. It is inexpensive (prototype cost $\approx$\$10,000 US, not including the digital frequency synthesizer, PC, or DAQ board).

The original, simpler design had noise levels of 970 Hz that corresponded[8] to uncertainties in lifetime of 1.7 ps. We
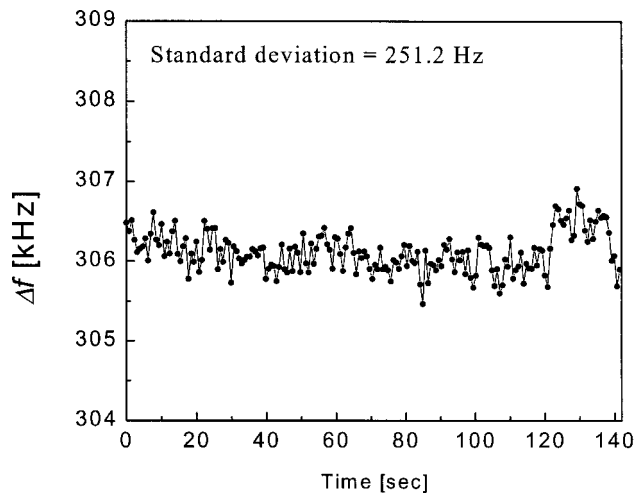
Fig. 6 Results from the experiment to estimate the lower limit on the prototype's noise levels. There is no cuvette containing fluorophore in the primary loop for this experiment.

showed here that the newer unit, with the secondary phase-feedback loop, has noise levels of 368 Hz. This corresponds to a capacity to discern very small changes in fluorescence lifetime (of the order of a picosecond, or $\delta\tau/\tau \sim 3 \times 10^{-4}$). The roughly 60% reduction in noise levels compensates for the 40% loss of frequency response to a given change in lifetime. Note, however, that the new design also has the potential for variable dynamic range. By reducing the gain of the dc amplifier (β), one can tune the relationship between $d\Omega$ and $d\tau$ shown in Eq. (7) to obtain smaller frequency responses to changes in lifetime.

Note that the sensor platform may not be the limiting factor in resolution of lifetimes. The closed-loop system itself is only half of a complete sensor system. The other half is the chemical and/or biological sensor component containing a fluorophore that changes its lifetime in response to an analyte. This component may be affected by many environmental factors such as changes in oxygen concentration or temperature. However, these kinds of effects are specific to the design of the molecular transduction system, and discussions of them would be appropriate only in the context of a particular design rather than a general presentation of a new instrumentation platform configuration.

The new configuration does not contain a long-λ-pass optical filter in the oscillatory loop. A secondary phase-feedback loop (containing an electronic phase detector and electronic phase shifter) must be added to provide the lifetime-dependent phase shift that enables the unit to function as a sensor platform. While this makes the system design much more complex, it provides some significant advantages. First, the reduction of signal losses in the oscillatory loop makes it easier to obtain self-oscillations. Second, the new phase-feedback mechanism acts as a stabilizing element, reducing noise levels.

Weak fluorescence sources could be addressed with either higher excitation light intensity or greater electronic gain in the main loop. There are limits to increasing the excitation light intensity as undesirable effects may be introduced, such as heating or bleaching. Increasing the electronic gain to too

great a level will also increase electronic noise and may result in a broader bandwidth of the self-oscillations. This is undesirable because it would reduce the precision of the frequency-counting method for lifetime measurements. The new configuration offers an alternative with smaller gain in the main loop.

The system, like its predecessor, is best suited for relative measurements. The constants Φ_{k_1} and Φ_{k_2} in Eq. (6) are due to discrete phase shifts in the optoelectronics, phase shifts that can change with different experiments (due to, for example, different gains on the resonance amplifier or different PMT bias voltages). These constants, of course, disappear with relative measurements, as can be seen in Eq. (7). While it is theoretically possible to come up with an exhaustive set of phase constants for a large array of experimental conditions and settings, such an endeavor would be time consuming at best. Furthermore, it would not really be necessary for chemical and biosensor applications, where the point is to measure a change in a parameter in response to a change in analyte concentration.

The components of the design presented here, like those of its predecessor, should be chosen for the lifetime range of the fluorophores used, meeting the condition ($\Omega\tau \sim 1$). The system will function outside of this window, but with reduced sensitivity. This places practical limits on the range of fluorophore lifetimes that can be used with this detection scheme. For example, lifetimes of the order of microseconds would require delay line lengths L of the order of kilometers, which would result in significant signal losses for visible or UV light.[8] However, lifetimes shorter than nanoseconds would be fine, provided the system were constructed with optoelectronic components capable of handling higher modulation frequencies. Components for much higher frequencies are available, including blue diode lasers which have been used with gigahertz-regime modulation spectroscopy experiments.[20]

References

1. M. Sekar, P. Hampton, T. Buranda, and G. P. Lopez, "Multifunctional monolayer assemblies for reversible direct fluorescence transduction of protein-ligand interactions at surfaces," *J. Am. Chem. Soc.* **121**, 5135–5141 (1999).
2. R. A. Agbaria, P. B. Oldham, M. McCarroll, L. B. McGown, and I. M. Warner, "Molecular fluorescence, phosphorescence, and chemiluminescence spectrometry," *Anal. Chem.* **74**, 3952–3962 (2002).
3. H. Szmancinski and J. R. Lakowicz, "Fluorescence lifetime-based sensing and imaging," *Sens. Actuat. B* **29**, 16–24 (1995).
4. J. Slavik, "Theory of fluorescence," Chap. 3 in *Fluorescent Probes in Cellular and Molecular Biology*, pp. 38–69, CRC Press, Ann Arbor, MI (1994).
5. S. B. Bambot, R. Holavanahali, J. R. Lackowicz, G. M. Carter, and G. Rao, "Phase fluorometric sterilizable optical oxygen sensor," *Biotechnol. Bioeng.* **43**, 1139–1145 (1994).
6. E. Rabinovich, M. J. O'Brien, S. R. J. Brueck, and G. P. Lopez, "Phase-sensitive multichannel detection system for chemical and biosensor arrays and fluorescence lifetime-based imaging," *Rev. Sci. Instrum.* **71**, 522–529 (2000).
7. M. J. O'Brien, E. Rabinovich, T. Svimonishvilli, S. R. J. Brueck, and G. P. Lopez, "Optoelectronic closed loop auto-oscillator for fluorescence lifetime detection: a new fluorimetry technique with applications to chemical biosensors," *Proc. SPIE* **4263**, 121–128 (2001).
8. M. J. O'Brien, E. Rabinovich, S. R. J. Brueck, and G. P. Lopez,

"Technique for detecting changes in fluorescence lifetime by means of optoelectronic circuit auto-oscillation," *Opt. Lett.* **26**, 1256–1258 (2001).

9. V. Vadde and V. Srinivas, "A closed-loop scheme for phase-sensitive fluorometry," *Rev. Sci. Instrum.* **66**, 3750–3754 (1995).

10. M. Nakazawa, T. Nakashima, and M. J. Tokuda, "An optoelectronic self-oscillatory circuit with an optical fiber delayed feedback and its injection locking technique," *J. Lightwave Technol.* **2**, 719–729 (1984).

11. T. V. Babkina, V. D. Burkov, V. V. Grigorants, A. F. Dashkin, and A. M. Radul, "A self-excited oscillator employing a fiber-optic delay line as a potential displacement sensor," *Telecommun. Radio Eng. (Engl. Transl.)* **46**, 118–121 (1991).

12. E. M. Rabinovich, C. L. Littler, J. M. Kowalski, and D. L. Maxson, "Remote vibration sensing using a radio-frequency auto-oscillatory opto-electronic circuit with fibre-optical delay line," *Meas. Sci. Technol.* **6**, 1407–1412 (1995).

13. J. Slavik, "Fluorescent labels," Chap. 9 in *Fluorescent Probes in Cellular and Molecular Biology*, pp. 242–268, CRC Press, Ann Arbor, MI (1994).

14. T. Buranda, G. P. Lopez, J. Keij, R. Harris, and L. A. Sklar, "Peptides, antibodies, and FRET on beads in flow cytometry: a model system using fluoresceinated and biotinylated beta-endorphin," *Cytometry* **37**, 21–31 (1999).

15. V. H. Perez-Luna, S. Yang, E. M. Rabinovich, T. Buranda, L. A. Sklar, P. D. Hampton, and G. P. Lopez, "Fluorescence biosensing strategy based on energy transfer between fluorescently labeled receptors and a metallic surface," *Biosens. Bioelectron.* **17**, 71–78 (2002).

16. P. Herman, B. P. Maliwal, H. J. Lin, and J. R. Lakowicz, "Frequency-domain fluorescence microscopy with the LED as a light source," *J. Microsc.* **203**, 176–181 (2001).

17. F. M. Mims, *Engineer's Mini-Notebook: Op Amp IC Circuits*, 2nd ed., Radio-Shack (1997).

18. A. J. Garcia, Chap. 5 in *Numerical Methods for Physicists*, pp. 119–161, Prentice-Hall, Englewood Cliffs, NJ (1994).

19. E. M. Rabinovich, T. Svimonishvili, M. J. O'Brien, S. R. J. Brueck, and G. P. Lopez, "Development of a new detection technique for fluorescence lifetime based chemical/biological sensor arrays monitoring: dual closed-loop optoelectronic auto-oscillatory detection circuit," *Proc. SPIE* **4624**, 115–122 (2002).

20. U. Gustavson, G. Someslalean, J. Alnis, and S. Svanberg, "Frequency-modulation spectroscopy with blue diode lasers," *Appl. Opt.* **39**, 3774–3780 (2000).